alexpacini.com

# Next Generation of High Power Density On-Board Chargers for Electric Vehicle Systems

A. Pacini, M. J. Kasper, A. Pevere, and G. Deboy

*Author Accepted Manuscript*

**To cite this version:**

A. Pacini, M. J. Kasper, A. Pevere, and G. Deboy, "Next Generation of High Power Density On-Board Chargers for Electric Vehicle Systems," in *2023 22nd International Symposium on Power Electronics (Ee)*, Oct. 2023, doi: 10.1109/Ee59906.2023.10346098.

```
@inproceedings{Pacini_2023_Ee_NextGenerationHighPowerDensity,
  author    = {Pacini, A. and Kasper, M.J. and Pevere, A. and Deboy, G.},
  title     = {Next Generation of High Power Density On-Board Chargers for Electric Vehicle
               Systems},
  booktitle = {2023 22nd International Symposium on Power Electronics (Ee)},
  year      = {2023},
  month     = oct,
  doi       = {10.1109/Ee59906.2023.10346098}
}
```

© 2023 IEEE. Personal use of this material is permitted. Permission from IEEE must be obtained for all other uses, in any current or future media, including reprinting/republishing this material for advertising or promotional purposes, creating new collective works, for resale or redistribution to servers or lists, or reuse of any copyrighted component of this work in other works.

# Next Generation of High Power Density On-board Chargers for Electric Vehicle Systems

Alex Pacini, Matthias J. Kasper, Alessandro Pevere, and Gerald Deboy
*Infineon Technologies Austria AG*
Siemensstr. 2, 9500 Villach, Austria
Email: {alex.pacini, matthias.kasper, alessandro.pevere, gerald.deboy}@infineon.com

***Abstract*—Electric vehicles are becoming increasingly popular, which has led to higher demands for on-board chargers (OBCs) that have to be compact, efficient, and compatible with different power systems worldwide. Currently, the state-of-the-art solution involves a phase-modular design, but this has limitations in terms of achievable power density due to the large number of components required. To achieve higher power density, the next generation of OBCs are transitioning to true three-phase topologies like the B6/B8 topology, which use 1200V-rated SiC MOSFETs. Additionally, multi-level topologies employing 600V-rated GaN HEMTs have been identified as a way to achieve further improvements in power density.**

**This paper shows two possible options for future OBCs to achieve the next level of power density: Non-isolated OBCs and single-stage power conversion enabled by monolithic bi-directional GaN HEMTs. These two different approaches are evaluated with respect to the single- and three-phase power processing requirements for worldwide compatibility, as well as the upcoming trend towards bi-directional power flow capability for V2x applications.**

***Index Terms*—Electric Vehicles, OBC, SiC MOSFETs, GaN HEMTs, BDS, Non Isolated OBC**

## I. Introduction

The on-going trend of electrification in the personal mobility sector has led to a significant increase of semiconductor content in cars. Among the fastest growing applications for power semiconductor devices are the traction inverter, on-board charging (OBC) equipment, and DC/DC converters that connect high-voltage and low-voltage batteries within electric cars (EVs). By employing innovative topologies and modulation schemes, system-level differentiation and value can be created, which can be further enhanced by selecting appropriate wide band-gap power devices.

This article focuses on alternative options for future on-board chargers to achieve the next level of power density. We will start with an overview of state-of-the-art solutions in **Sec. II**, present non-isolated chargers and technology/application aspects of upcoming bi-directional GaN switches in **Sec. III** and **Sec. IV**, respectively. We will continue showing pahse-modular and ture three-phase single-stage architectures in **Sec. V** and will close discussing power density challenges and their respective solutions for combined single- and three-phase OBCs in **Sec. VI**.

979-8-3503-4317-5123/$31.00 ©2023 IEEE

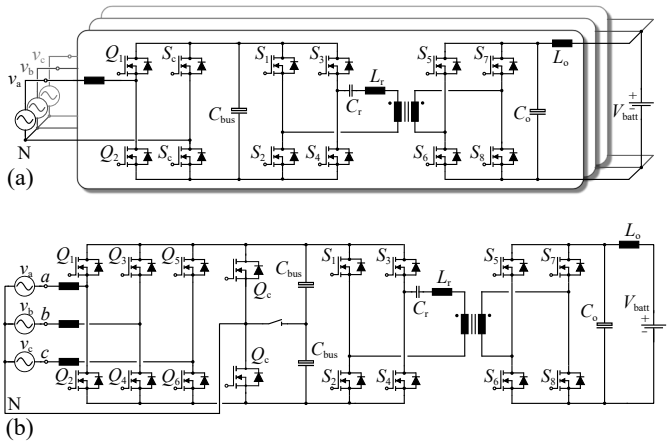



**Fig. 1.** Overview of state-of-the-art on-board charger solutions: (a) Phase-modular solution where each phase module contains a bridge-less PFC with subsequent DC/DC converter, and (b) true three-phase unified B6/B8 topology.

## II. State-of-the-Art Solutions

In this section, an overview of state-of-the-art OBC solutions is provided. Currently, most EVs on the road are equipped with phase-modular solutions for their simplicity to cope with world wide grid compatibility. For the next generation of OBCs with higher power densities, true three-phase topologies are under development.

### A. Phase-Modular Systems

The conversion stages of phase-modular systems (shown in **Fig. 1(a)**) operate independently on each of the three line-to-neutral connections. This provides the highest degree of flexibility for both true three-phase grids and single-phase installations, including 240 V AC US split-phase, which enables the delivery of the rated power in all scenarios, if required. Each of the three power converters has an AC/DC power factor correction (PFC) circuit, a DC-link, and a subsequent DC/DC converter for galvanic isolation and output voltage regulation, as all of the power stages are referenced to the neutral line potential.

A typical implementation using a bridge-less PFC stage and an LLC converter as isolating DC/DC stage is shown in **Fig. 1(a)**. The efficiency of this solution reaches up to 95 %

with power densities of 1 kW/l to 1.5 kW/l. The PFC stage runs typically in Continous Conduction Mode (CCM) at switching frequencies of 20 to 60 kHz. At the lower end of switching frequencies IGBTs with anti-parallel Si or SiC Schottky diodes are used as switches $Q_1$ to $Q_4$, whereas SiC MOSFETs or GaN HEMTs create value at the upper end of switching frequencies, e.g. above 100 kHz. The unfolding switches $S_c$ may be based on low-ohmic MOSFETs that are cost-optimized for lowest conduction losses, such as the CoolMOS™ S7 series.

The shift towards partial or full-rated bi-directional power flow requirements for supporting vehicle-to-load (V2L) and/or Vehicle-to-Vehicle (V2V) applications can be achieved through the phase-modular concept by using active switches as rectification elements on the battery side, specifically $S_5$ to $S_8$. However, due to the potential hard commutation of the reverse conducting body diodes, such as in over-resonant operation of the LLC, it is recommended to use SiC or GaN devices as synchronous rectification elements. Moreover, to support full bi-directional power flow, the DC/DC converter must be transformed into a symmetrical converter architecture, such as a CLLC converter or a dual-active bridge (DAB) converter. Whereas, in the PFC stage, the bridge-less totem-pole architecture is already bi-directional by nature, as long as active devices are used in the unfolder bridge-leg ($S_c$) in place of diodes.

As the battery voltages transition more and more to the 800 V architecture, the relatively low DC-link voltage of 400 V must be increased by corresponding transformer ratios to output voltages that are typically twice the input voltage with 1200 V-rated semiconductors on the secondary side. It is worth noting that the broad voltage range of 800 V batteries, which can cover a factor of $> 2$ between a fully charged and a fully discharged battery, pushes the classic frequency modulation of the LLC converter to its limits. Specifically, very low battery voltages result in strong over-resonant operation, which can lead to thermal issues in the converter.

The simplicity of the phase-modular concept, however, comes at the expense of a high count of active and passive components, which limits the achievable power density. This can be overcome by transitioning to true three-phase topologies, which are analyzed in the following section.

### *B. True three-phase Bi-directional Architectures*

Typically, a true three-phase architecture employs a two-stage approach for implementing the bi-directional on-board charger, comprising of one direct three-phase PFC and one DC/DC converter, as depicted in **Fig. 1(b)**. In comparison to the phase-modular solution, the true three-phase charger offers higher power density with fewer components and transformers, and can be extended to 800 V batteries.

Upcoming on-board chargers require the *unbalanced three-phases charging* mode, which involves drawing varying power levels from the three phase of the mains. The standard three-wire B6 topology (without a neutral line connection) is unable to satisfy this requirement as it necessitates the sum of the three phase currents to be zero. In order to facilitate unbalanced three-phase charging, the neutral line is connected to the midpoint of the split-capacitor DC-link to create a four-wire B6 PFC.

The availability of a three-phase grid can be limited, particularly when charging at home or depending on the country in which the EV is located. Therefore, a universal OBC that is compatible with both single- and three-phase grids for worldwide use has significant commercial value. The four-wire B6 is compatible with single-phase operation, but its primary disadvantage is the significant line frequency ripple that occurs at the split capacitors of the dc-link due to the use of only one capacitor for each half line cycle. As a result, large DC-link capacitors with high rms-current ratings have to be installed.

To overcome this issue, the B8 topology has been introduced, where an additional low-frequency half-bridge leg is connected to the neutral line to enable full-bridge operation with single-phase grids. The DC-link capacitors now only experience a current ripple at twice the line frequency and with lower amplitude. The B8 topology, however, is unable to support the unbalanced three-phase charging requirement as there is no connection between the neutral line and the midpoint of the dc-link capacitors in three-phase operation. Therefore, a unified B6/B8 topology has been proposed [1] to enable both three-phase and single-phase operation, as well as operation under unbalanced three-phase conditions, as in **Fig. 1(b)**. The unified B6/B8 incorporates a relay between the mid-point of the low-frequency bridge-leg (i.e. connected to neutral line) and the dc-link mid-point. By opening the relay during single-phase operation and closing it during three-phase mode, unbalanced three-phase charging is supported while preventing high ripple on the dc-link capacitors during single phase operation.

For output voltages above peak line-to-line voltage, the use of semiconductors with $\geq 900$ V voltage rating, such as 1200 V SiC MOSFETs, is required for the B6/B8 converter.

Even though the transition from phase-modular solutions to true-three phase solutions allows to increase the power density from previously 1-1.5 kW/l to around 3 kW/l, further power density improvements are difficult to achieve due to the inherently limited switching frequencies of 1200 V-rated devices and the presence of only 2-level waveforms. This leads to large voltage-time areas across the magnetic components and subsequently large volumes of the passive components. These limitations can be overcome with multi-level architectures, as described in the next section.

### *C. Multi-Levels Three-Phase Architectures*

The advantages of multi-level topologies are on the one hand the usage of lower-rated semiconductors, e.g. 600/650 V devices for DC-links with 800 V. This opens up the possibility to use cost-effective lateral GaN-on-Si HEMTs with better figure-of-merits than Si or SiC devices. But the impact of transitioning from 2-level to multi-level topologies goes beyond the bare semiconductors. Multi-level topologies, on the other hand, also provide a larger number of voltage levels

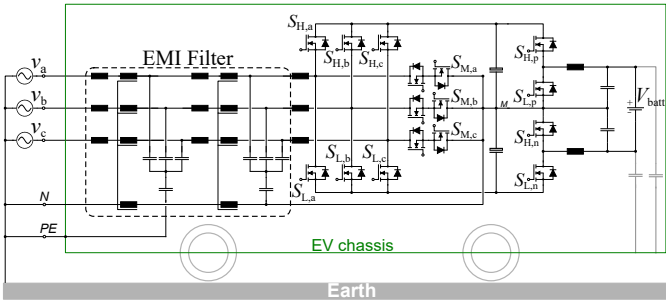



**Fig. 2.** Non-isolated on-board charger based on a T-type rectifier and two stacked buck converters.

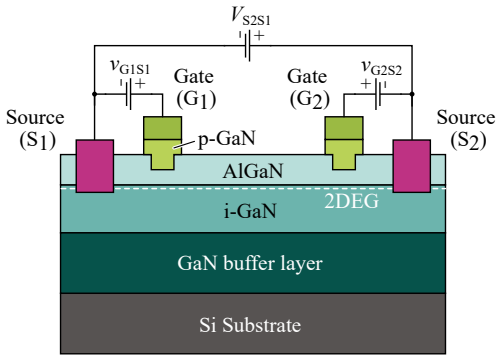



**Fig. 3.** Cross-section view of a normally-off monolithic bi-directional GaN-on-Si HEMT in common-drain configuration.

for PWM operation. In PFCs, prominent candidates of 3-level topologies are the flying capacitor topology, T-type, and different NPC derivates [2]. Out of these, the flying capacitor as well as the double-frequency active neutral point clamp (DF-ANPC) topology provide in addition also a frequency multiplication, which leads to a reduction of the input current ripple by a factor of $1/N_{\text{cells}}^2$, with $N_{\text{cells}}$ being the number of switching cells (i.e. $N_{\text{cells}} = N_{\text{levels}} - 1$). Thus, in these two 3-level topologies, the input current ripple is only $1/4$ of the current ripple of a 2-level topology. This advantage can be used to either shrink the size of the passive components, or to reduce the switching frequency of the employed semiconductors to lower the switching losses. Beyond that, multi-level topologies also offer a better heat-spreading as the current and/or voltage stress is spread among multiple devices [3].

In isolated DC/DC converters the transformer is typically the largest contributor to the overall volume and losses. Splitting up a single DC/DC converter with one large transformer into multiple DC/DC stages with smaller transformers is only leading to lower overall volumes and losses when thermal limitations of the transformers is reached, e.g. at high switching frequencies [2].

## III. Non-Isolated On-board Chargers

The increasing performance requirements for on-board power converters have encouraged an additional alternative research trend from traditional isolated battery chargers to non-isolated on-board chargers (NIOBC). Both, car manufacturers and academia, are heavily investigating this topic, since the removal of the bulky isolation transformer would allow to save losses, cost, and volume. An example of non-isolated on-board charger is presented in **Fig. 2**, where the AC/DC stage is a three-phase four-wire boost rectifier based on the T-type topology, in which each leg is implemented by two 1200 V MOSFETs plus two switches in back-to-back configuration for the connection with the split-capacitor mid-point. The DC/DC stage is realized with two cascaded buck converters, one connected to the positive half DC-link and the other to the negative. The mid-point of the DC-link capacitors is connected to neutral in order to stabilize the potential of the output capacitors and thus also the battery potentials with respect to protective earth. This connection also enables single-phase operation and operation with unbalanced loading of the phases in 3-phase operation. NIOBCs require careful design and system control to minimize leakage and touch currents through the parasitic capacitances between HV battery poles (positive and negative) and protective earth (PE) (grey capacitors in **Fig. 2**), which are limited by regulation to a few mA [4], [5].

## IV. Monolithic Bi-Directional GaN Switches

Most commercially available GaN HEMTs are grown by means of metal organic chemical vapor deposition (MOCVD) on a Silicon substrate, which is the most cost effective way of producing GaN devices in high volume. Unlike vertical Si Superjunction MOSFETs or SiC Trench MOSFETs, GaN-on-Si HEMTs are lateral devices, where the source, gate, and drain contacts are on the same side of the wafer. The superior performance of GaN HEMTs comes from the high electron mobility and electron density of the 2-dimensional electron gas (2DEG) which is formed at the AlGan/GaN heterojunction due to spontaneous and piezoelectric polarizations, and spans between the source and drain contacts **Fig. 3**. Such a device is by nature a normally-on device, which however is less suitable for power electronic applications, in which at all conditions e.g. during start-up and/or loss of auxiliary power, a safe operation has to be guaranteed. This has triggered the development of normally-off GaN HEMTs. One possible way to achieve that is by implementing a p-GaN layer below the gate that lifts the band diagram to higher energies and thus also the threshold voltage to positive levels [6]. Such a device is in the off-state (i.e. with zero or negative gate voltage) capable of blocking an applied voltage in drain-to-source direction, while a negative drain-source voltage can not be blocked, as it will lift the gate potential above the threshold and turn-on the device.

In order to create a device that can block voltages and conduct currents in both directions, in lateral GaN HEMTs a second gate module can fairly easy be implemented close to (what was previously) the drain contact. This creates a normally-off monolithic bi-directional common-drain switch (M-BDS), which utilizes the same drift-region in both directions. This is an improvement of chip area by a factor of four compared to the back-to-back arrangement of uni-

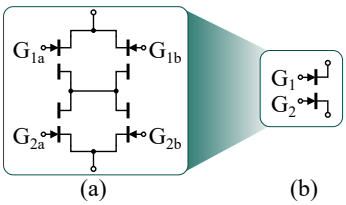



**Fig. 4.** Chip area comparison of a bi-directional switch consisting of (a) four uni-directional devices in back-to-back configuration or (b) a monolithic bi-directional switch (MBDS) with the same effective $R_{\mathrm{DS,on}}$.

directional power devices, since such an arrangement leads to twice the on-state resistance and needs another parallel arrangement to achieve the same $R_{\mathrm{DS,on}}$ as one individual device (cf. **Fig. 4**). Manufacturing an M-BDS switch on a vertical device structure is much more challenging, as the https://www.overleaf.com/project/650b38b062f18f3424fba0dfwafer would have to be processed on both sides to implement the second gate module close to the bottom contact [7].

The benefits of M-BDS GaN switches have been demonstrated already in several use cases, which can be classified as

- replacement for back-to-back switches in T-type / Vienna Rectifier systems (cf. **Fig. 2**) [8], HERIC inverters [9], and H4 PFCs [10],
- current source inverters / rectifiers [11],
- direct and indirect AC/AC matrix converters [12], and
- single-stage isolated AC/DC power conversion.

Particularly the last class of topologies has attracted a lot of research lately, as it allows to merge the PFC and the high-frequency isolation stage into a single conversion stage. This is not only creating savings in volume and losses but also in cost. In the next section, the concept of single stage power conversion will be examined more closely within the scope of on-board chargers.

## V. Single-Stage On-board Chargers

The M-BDS GaN switches allow to interface the primary side of the HF isolation transformer directly with the AC input voltage, thus providing PFC functionality and galvanic isolation in a single conversion stage of so-called cycloconverters. This can be applied to both, phase modular as well as true three phase systems (cf. **Fig. 5**). An example of the former is shown in **Fig. 5(a)** [13], which converts the AC input voltage of each phase similar to a DAB to a constant isolated output voltage, where the pulsating powers of the three phases are added together to yield a constant output power. This system structure provides the advantages of using only 600/650 V rated semiconductor devices and of an inherent compatibility with 1-$\phi$ and 3-$\phi$ grids, but comes at the penalty of higher component count.

An example of a true three phase system is shown in **Fig. 5(b)** [14] which is also controlled like a DAB. The modulation scheme is however more complex, since at any time instant only one phase-to-phase voltage can be applied

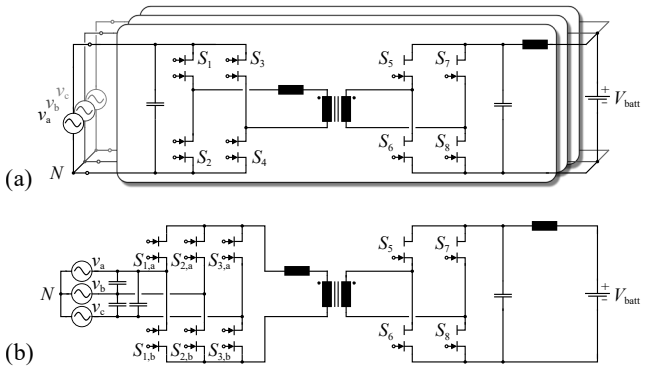



**Fig. 5.** Single-stage DAB-type cycloconverter solutions with MBDS devices for future on-board charger generations: (a) Phase-modular and (b) true three-phase topology.

to the primary side of the HF transformer. Thus, the control degrees of freedom comprise not only the DAB-typical degrees of freedom like the duty cycle of the primary and secondary sides with the phase shift and the switching frequency, but also the choice of which phase-to-phase voltages are selected for how long in each half-wave. This leads to a complex control pattern optimization problem and is in the specific case of [14] solved by implementing a large look-up table with 27'000 entries. Furthermore, for 1-$\phi$ compatibility a fourth bridge-leg for connecting the neutral wire to the transformer as well as a change of control is required. On the upside, a lower component count can be named. The voltage rating of the M-BDS devices in such a system needs to be high enough to block line-to-line voltages (i.e. $230\,\mathrm{V_{rms}} \cdot \sqrt{2} \cdot \sqrt{3} \approx 563\,\mathrm{V}$) which means that (including some margin for grid variations) a voltage rating of around 800 V to 900 V is required. This is substantially lower than the 1200 V voltage rating required in typical two-stage true 3-phase systems and is easier achievable with the standard GaN-on-Si manufacturing processes than 1200 V GaN devices. In order to make the topology of **Fig. 5(b)** compatible with single phase grids, a fourth bridge-leg connecting to the neutral wire has to be added to the primary side bridge-legs.

## VI. High Power Density Challenges for Combined Single- and Three-Phase OBCs

Since the three-phase grid might not be always available, especially when charging at home or depending on which country the EV is charging, it is commercially valuable to design a universal OBC that is compatible with both single- and three-phase grids for worldwide use. This requirement is significantly increasing the design challenges of the OBC. In the next subsections, two important power density limitation factors in single phase operation will be presented and possible solutions will be addressed.

### A. DC-Link Voltage Balancer

In a non-isolated OBC, the three-phase four-wire rectifier is a standard solution of the AC/DC stage, as already discussed in **Sec. III**, with a split DC-link where the midpoint M

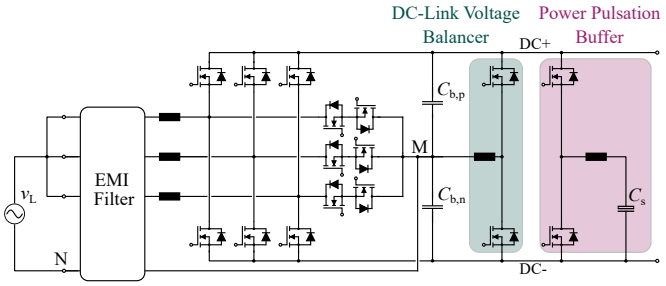



**Fig. 6.** Three-phase T-type rectifier operating in single-phase grid with DC-link voltage balancer and power pulsation buffer circuits.

is connected to neutral N of the grid (see **Fig. 6**). The main disadvantage in single-phase operation is the large line-frequency ripple at the dc-link split capacitors due to the utilization of only one capacitor for each half line-cycle [2].

The most common approach to mitigate this issue is to oversized the dc-link capacitors $C_{b_p}$ and $C_{b_n}$ of **Fig. 6** in terms of ripple current capability, compromising the power density of the converter.

An alternative method is to add an active balancing circuit, also known as "DC-link voltage balancer", that symmetrizes the voltages across the two spit capacitors $C_{b_p}$ and $C_{b_n}$ [5]. The added circuit is a half-bridge with its mid-point connected to the mid-point of the split capacitors through an inductor, as shown in **Fig. 6**. The voltage balancer is typically working with 50% duty cycle since it only has to re-balance the line frequency current component in the dc-link split capacitors. The balancer current has to be the same of the phase input current in order to avoid current flowing into the split capacitors. The current ripple of the balancer depends on inductance value and switching frequency. The balancer switches need to block the full dc-link voltage.

### *B. Power Pulsation Buffer*

In single-phase operation, for both isolated and non-isolated OBCs, an energy storage device is also necessary for handling the instantaneous imbalance of the input and output power.

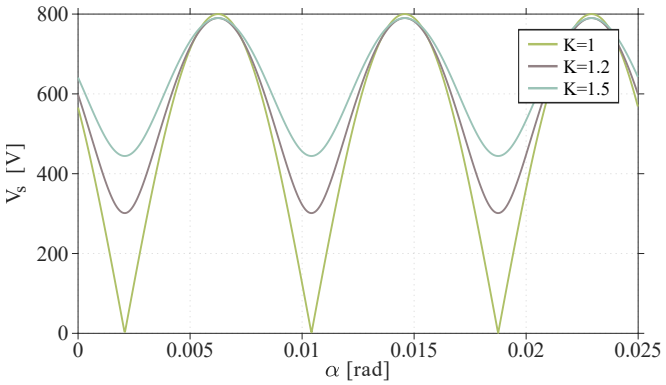



**Fig. 7.** Power pulsation buffer capacitor voltage for different capacitance values as a function of parameter $K$, denoting the design margin.

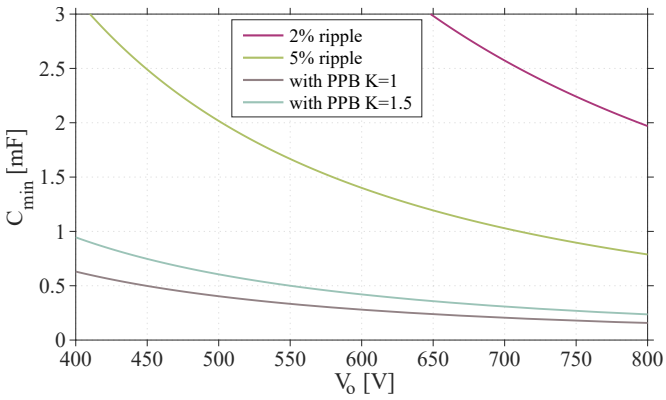



**Fig. 8.** Minimum capacitance value as a function of the DC-link voltage and the parameter K with and without power pulsation buffer.

Without this device, the instantaneous input/output power imbalance induces a high double-line frequency ripple across the load. The power imbalance is reduced by storing energy during periods when the input power is higher than the output power and supplying energy during periods when the input power is lower than the output power. This is typically implemented with the equivalent capacitor $C_b$ between DC+ and DC- terminals of the AC/DC stage output (i.e. series connected capacitors $C_{b_p}$ and $C_{b_n}$ in the circuit of **Fig. 6**).

Due to the low frequency ripple (100/120 Hz), the required capacitance value of $C_b$ is usually implemented with relatively large aluminum electrolytic capacitors, negatively impacting power density and lifetime of the overall power conversion system. The minimum bulk capacitance value $C_{b_{min}}$ also depends on the allowed voltage ripple between DC+ and DC- and can be approximated by the following equation:

$$C_{b_{min}} = \frac{V_{in} I_{in}}{2\omega \Delta v_o^{\%} V_o^2} \tag{1}$$

where $V_{in}$ and $I_{in}$ are the rms input voltage and current values, $\omega$ is the angular line frequency, $V_o$ is the voltage between DC+ and DC- and $\Delta v_o^{\%}$ is the voltage ripple, normalized to $V_o$. Since the allowable voltage ripple on the DC-link is limited, rather large capacitance values result. As an alternative way to solve this problem, an external converter can be added in parallel to the rectifier output as shown in **Fig. 6**. This active circuit, also referred in literature as active power decoupling circuit or power pulsation buffer (PPB) [15], includes switches plus storage elements, i.e. inductors and capacitors. By properly controlling the on/off states of the switches, the second-order ripple pulsation is moved from the DC-link to the energy of storage element $C_s$ of the PPB circuit, while keeping the voltage across $C_b$ almost constant. This method greatly reduces converter volume and prolongs the service life of the system. Among the most common PPB architectures, the bi-directional buck topology is the most popular for its low component count and voltage stress, as well as good performance. The minimum storage capacitance

value for a buck-type PPB can be written as:

$$C_{s_{min}} = \frac{2V_{in}I_{in}}{\omega V_o^2} \tag{2}$$

Typically, a certain design margin $K$ is considered, such that $C_s = KC_{s_{min}}$, i.e. the storage capacitance is higher than the calculated minimum value by a factor $K$. This will have also an impact on the twice line frequency ripple that the storage capacitor will experience, as shown in **Fig. 7**.

The ratio between the required bulk capacitance for a standard rectifier and the required storage capacitance in PPB system can be expressed as:

$$r_C = \frac{C_{b_{min}}}{C_s} = \frac{1}{4K\Delta v_o^{\%}} \tag{3}$$

**Fig. 8** presents a comparison of the minimum capacitance values for rectifiers with and without power pulsation buffer as a function of the DC-value of the bulk voltage. Even if a certain margin from its minimum value is considered, e.g. $K = 1.5$, the storage capacitance requirement is considerably lower than the required bulk capacitance of a standard PFC even with a large voltage ripple, e.g. $v_o^{\%} = 5\%$. It is also clear from (3) that the minimum capacitance ratio depends only on the PPB margin factor and the allowed voltage ripple on the bulk capacitor and not on the absolute value of the DC-link voltage.

## VII. Conclusions and Outlook

The increasing requirements on on-board chargers with respect to power level, power density, weight, bi-directionality, and world-wide grid compatibility is driving the development of future on-board generations. The wide-spread solutions of phase-modular topologies in current EVs are increasingly becoming replaced by true three-phase topologies with 1200 V rated SiC MOSFETs due to their higher power density and lower component count. Further improvements towards higher power density can be achieved with multi-level topologies leveraging the benefits of better FoM semiconductors and smaller voltage-time areas seen by the magnetic components. For even further power density improvements, radically different concepts have to be considered: non-isolated or single-stage on-board chargers. In the former one, limiting the parasitic common-mode currents through the parasitic battery capacitances to only a few mA in all operating modes is the largest challenge. For the latter one, the emergence of cost-effective M-BDS GaN devices has revived a research trend of these solutions that were previously commercially not attractive with a back-to-back arrangement of uni-directional semiconductors.

Beyond the scope of this article are considerations among developers to remove the on-board charger as it is currently known. By using off-board DC-chargers, residential houses with photovoltaic panels and battery storage systems can create a DC-coupled system where also the EV-charger is integrated. By having the charging electronics permanently installed in a fixed location, guaranteeing the compliance with local grid norms becomes significantly easier. The on-board charger would only be needed in case of emergencies and could be sized for single-phase operation with a few kilowatts. Other concepts favor the integration of the battery charger electronic into the motor inverter, which is already rated for several hundreds of kW [16].

## References


[1] P. Papamanolis, D. Bortis, F. Krismer, D. Menzi, and J. W. Kolar, "New EV battery charger PFC rectifier front-end allowing full power delivery in 3-phase and 1-phase operation," *Electronics*, vol. 10, no. 17, p. 2069, 2021.

[2] M. J. Kasper, A. Pacini, A. Pevere, J. A. Anderson, and G. Deboy, "Concepts and matching power semiconductor devices for compact on-board chargers," in *2023 IEEE 17th International Conference on Compatibility, Power Electronics and Power Engineering (CPE-POWERENG)*, 2023, pp. 1–7.

[3] M. Kasper, D. Bortis, and J. W. Kolar, "Scaling and balancing of multi-cell converters," in *2014 International Power Electronics Conference (IPEC-Hiroshima 2014 - ECCE ASIA)*, 2014, pp. 2079–2086.

[4] Y. Zhang, G. Yang, X. He, M. Elshaer, W. Perdikakis, H. Li, C. Yao, J. Wang, K. Zou, Z. Xu, and C. Chen, "Leakage current issue of non-isolated integrated chargers for electric vehicles," in *2018 IEEE Energy Conversion Congress and Exposition (ECCE)*, 2018, pp. 1221–1227.

[5] B. Strothmann, F. Schafmeister, and J. Böcker, "Common-Mode-Free Bidirectional Three-Phase PFC-Rectifier for Non-Isolated EV Charger," in *2021 IEEE Applied Power Electronics Conference and Exposition (APEC)*, 2021, pp. 2783–2790.

[6] M. Meneghini, C. De Santi, I. Abid, M. Buffolo, M. Cioni, R. A. Khadar, L. Nela, N. Zagni, A. Chini, F. Medjdoub, G. Meneghesso, G. Verzellesi, E. Zanoni, and E. Matioli, "GaN-based power devices: Physics, reliability, and perspectives," *Journal of Applied Physics*, vol. 130, no. 18, p. 181101, 11 2021.

[7] S. Chowdhury, C. W. Hitchcock, Z. Stum, R. P. Dahal, I. B. Bhat, and T. P. Chow, "Operating principles, design considerations, and experimental characteristics of high-voltage 4h-sic bidirectional igbts," *IEEE Transactions on Electron Devices*, vol. 64, no. 3, pp. 888–896, 2017.

[8] F. Vollmaier, N. Nain, J. Huber, J. W. Kolar, K. K. Leong, and B. Pandya, "Performance evaluation of future t-type pfc rectifier and inverter systems with monolithic bidirectional 600 v gan switches," in *2021 IEEE Energy Conversion Congress and Exposition (ECCE)*, 2021, pp. 5297–5304.

[9] H. Schmidt, C. Siedle, and J. Ketterer, "DC/AC converter to convert direct electric voltage into alternating voltage or into alternating current," Patent US 7.046,534 B2.

[10] H. Gan, H. Jin, and J. Zeng, "Bridgeless PFC circuit system having current sensing circuit and controlling method thereof," Patent US 8,773,879 B2.

[11] N. Nain, J. Huber, and J. W. Kolar, "Comparative evaluation of three-phase ac-ac voltage/current-source converter systems employing latest gan power transistor technology," in *2022 International Power Electronics Conference (IPEC-Himeji 2022- ECCE Asia)*, 2022, pp. 1726–1733.

[12] L. Huber, D. Borojevic, and N. Burany, "Voltage space vector based pwm control of forced commutated cycloconverters," in *15th Annual Conference of IEEE Industrial Electronics Society*, 1989, pp. 106–111 vol.1.

[13] F. Jauch, "Medium Voltage AC-DC Converter Systems for Ultra-Fast Charging Stations for Electric Vehicles," Ph.D. dissertation, ETH Zurich, 2016.

[14] L. Schrittwieser, "Ultra-Efficient Three-Phase Buck-Type PFC Rectifier Systems," Ph.D. dissertation, ETH Zurich, 2018.

[15] A. Pevere, A. Rossi, and R. Petrella, "Analysis and control of active ripple energy storage for single-phase pfc converters," in *PCIM Europe 2022; International Exhibition and Conference for Power Electronics, Intelligent Motion, Renewable Energy and Energy Management*, 2022, pp. 1–10.

[16] T. Na, X. Yuan, J. Tang, and Q. Zhang, "A review of on-board integrated electric vehicles charger and a new single-phase integrated charger," *CPSS Transactions on Power Electronics and Applications*, vol. 4, no. 4, pp. 288–298, 2019.